Section:ResearchPaper

DEVELOPING A HYBRID APPROACH FOR ENHANCEDEARLY ACUTE GLAUCOMA SCREENING BY COMBINED DEEP LEARNING APPROACH

[1]**Santhosh S,** Research Scholar, Srinivas University, Mangalore, Assistant Prof. Dept. of ISE Nitte (Deemed to be University) NMAM Institute of Technology (NMAMIT) Nitte, India. santhosh.s@nitte.edu.in

[2]**Dr. D. Veerabhadra Babu,** Professor, Srinivas University, Mangalore, India. veerabhadra.durgam@gmail.com

[3]**Dr. Anoop B. K.,** Professor, Dept. of AIML, Srinivas Institute of Technology, Mangalore, India. dranoopbk@sitmng.ac.in, https://orcid.org/0000-0003-4288-5065

Abstract

Diagnosis and diagnosis of glaucoma progression remain difficult. Artificial intelligence-based techniques have the potential to improve and standardize glaucoma examination, however because of the multimodal and changeable nature of the diagnosis, developing these algorithms is difficult. Most algorithms are now focused on a single imaging modality, namely screening and diagnosis using fundus pictures or optical coherence tomography images. In our review of the literature, we found no research that evaluated the use of artificial intelligence for treatment response prediction, and no studies that conducted prospective testing of their algorithms. Another barrier to the development of artificial intelligence-based solutions is a lack of data and agreement on diagnostic criteria. Although research on the use of artificial intelligence for glaucoma is promising, more research is required to develop clinically usable tools. Current glaucoma detection convolutional neural networks (CNNs) are all based on spatial data embedded in an image. We created a hybrid CNN and recurrent neural network (RNN) that extracts not only the spatial but also the temporal characteristics encoded in a fundus image. A total of 1810 fundus photos and 295 fundus images were used to train a CNN and a CNN-LSTM-RNN combination. In differentiating glaucoma from healthy eyes, the combined CNN/RNN model achieved an average F-measure of 94.3%. A detecting system is required to aid in the early identification of glaucoma. The researchers propose employing deep learning technology to detect and forecast glaucoma before symptoms arise in this study. The results are contrasted with deep learning-based convolution neural network classification techniques. The suggested model has an accuracy of 98.21% when used for training and an accuracy of 96.34% when used for testing. According to all evaluations, the newly proposed paradigm is more effective than the one that is already in use.

KeyWords: Glaucoma, Artificial Intelligence, Deep Learning, Deep Convolution Neural Network, Recurrent Neural Network, Long Short-Term Memory.

1. INTRODUCTION

Glaucoma is a chronic, progressive optic neuropathy that causes the loss of retinal nerve fibers. Though asymptomatic in the early stages, it can lead to severe, permanent vision loss over time. As a result, early detection is critical. Glaucoma is the primary cause of irreversible blindness

worldwide, with a prevalence of 111.8 million expected by 2040[1][2]. There is a critical unmet need for improved screening and diagnosis; half of all glaucoma cases in the United States remain undetected.6 AI, and deep learning (DL) in particular, not only represents a potential solution to address this expanding need through scale screening, but also represents an opportunity for treatment and prognosis customization. Although AI has significant potential to affect glaucoma screening, diagnosis, and prediction, no algorithms can successfully meet these objectives. Several issues pertaining to model design for glaucoma use cases continue to be impediments to the development of clinically deployable algorithms. In many countries, comprehensive health screening programs, including screening fundus photography for early identification and prevention of majorities, have recently become more popular, and the incidental detection of abnormal fundus findings has also increased. A notable example of such findings that ophthalmologists pay attention to is large optic disc cupping or large cup-to-disc ratio (CDR) without RNFL defect (RNFLD). Furthermore, ophthalmologists meet such optic discs on a regular basis during fundus examinations, and optic discs with vertical CDR 0.6 are especially concerning because they may indicate glaucomatous optic disc destruction [3].

Even though some of these have been labelled as pseudo-glaucomatous physiologic large cups, which are thought to be normal variants, little is known about the long-term natural clinical course, and clinical guidelines for programmed follow-up surveillance tests for these eyes have not yet been proposed [4]. Many patients with large CDR without RNFLD have been routinely followed up on for an indefinite period under the condition of 'glaucoma-like disc' (GLD) or the diagnosis of glaucoma suspect, undergoing wasteful repetitive examinations such as disc photography, RNFL photography, optical coherence tomography (OCT), and automated perimetry. In contrast, some GLD patients acquire RNFLD and/or VF defect, allowing them to begin antiglaucoma drugs. As a result, if we can predict the development of glaucoma and identify personalized risk factors for glaucoma conversion in eyes with GLD, we can give everyone a tailored follow-up investigational plan. Fundus pictures give a 30-degree image of the ONH as well as the ability to assess several glaucoma-specific morphological features [5, 6], such as neuro-retinal rim loss and a higher cup-to-disc ratio [6].

Despite the computer-aided technique of objectively assessing these aspects, there is well-known inter- and intra-observer heterogeneity in processing ONH images [7]. Another significant drawback of single fundus imaging is that it does not detect signs associated with blood flow dysregulation, a well-known glaucoma phenomenon [8]. To address this constraint, a lot of recent research has focused on analyzing image sequences in search of blood flow markers. Temporal features such as changes in the amplitude of spontaneous venous pulsations (SVP) [9] and blood column variations [10] can be acquired by analyzing fundus videos, both of which have been connected to glaucoma [11][13]. For any approach to glaucoma assessment, it is critical to consider both spatial and temporal information. Computer-aided diagnostic (CAD) technologies are crucial in making an accurate, reliable, and timely diagnosis of glaucoma [14].

Recent developments in processing capacity have enabled the introduction of convolutional neural networks (CNN), which allow for the autonomous classification of glaucoma based on complex features extracted from hundreds of fundus pictures. The specificity and sensitivity of these models vary from 85 to 95%, with transfer-trained models outperforming native trained models in distinguishing glaucoma from healthy fundus images [15-17]. While these experimental results suggest that pre-trained CNNs can outperform untrained CNNs in diagnosing glaucomatous fundus images, the complexity of glaucoma pathology presents distinct hurdles for CNNs trained solely on fundus images. The retina was imaged using a fundus camera, which is commonly used by ophthalmologists. A retinal picture can be used to identify glaucoma and other eye problems. Glaucoma is the leading cause of blindness worldwide. Glaucoma alters the central cup region of

the ONH. These factors could be used to rule out glaucoma. The optic nerve head sends images from the retina to the brain. Look closely at the retina in Figure 1 to see what is known as a fundus. Glaucoma, a disorder that destroys the visual nerves, has no early warning signals, yet it eventually leads to blindness. The sooner glaucoma is discovered and treated, the greater the patient's chances of retaining vision in the affected eye. When glaucoma reaches a certain stage of progression, the optic cup is excavated. The "cupto-disc ratio" denotes the relationship between the optical cup and the optical disc. Ophthalmologists may utilise the CDR value to track the course of glaucoma. To obtain CDR from a retinal image, a two-step segmentation procedure is required. Up till the CDR is received, this process is continued. The most obvious sign of glaucoma development is frequently a progressive dimming or loss of peripheral vision. Here's just one illustration: Glaucoma, for instance, is referred to as "the wise one" even though it is also referred to as "the thief of eyesight" due to the harm it causes to patients' vision. When you are close to bright lights, it's conceivable that you will see a halo-like glow if you have high intraocular pressure. Blindness, eye discomfort, blurry vision (particularly in infants), violent vomiting, or feeling lightheaded are all potential side effects [18].

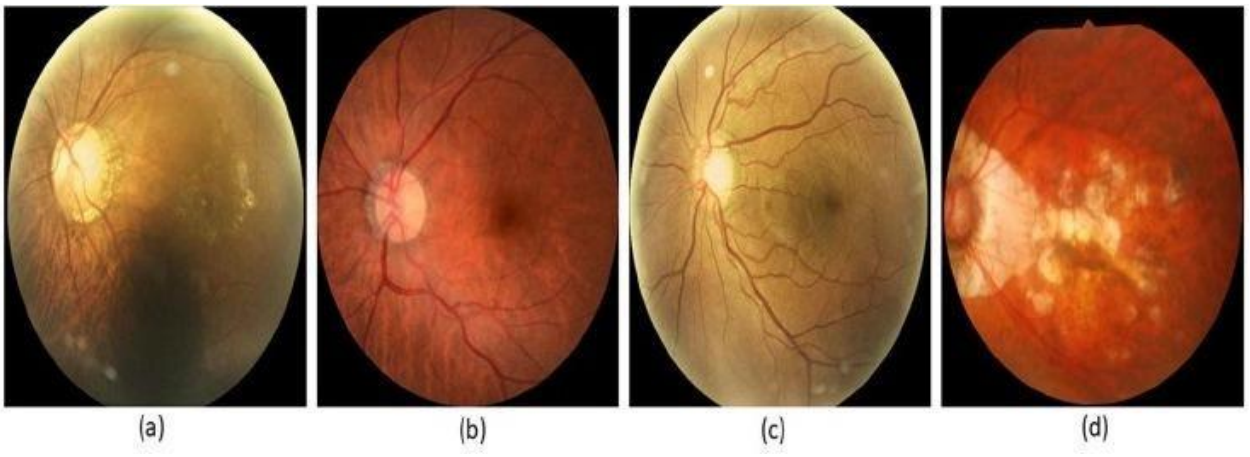

Fig. 1: Glaucoma images: (a) macular epiretinal membrane, (b) normal fundus, (c) mild nonproliferativeretinopathy, (d) pathological myopia.

The glaucoma dataset is utilised by the suggested deep learning model for analysing glaucoma images. In this design, a deep convolution neural network is combined with the RNN-LSTM model, which is sometimes referred to as a pretrained kind of transfer learning. It yields the segments and attributes of this model [19]. Images of a normal and glaucoma fundus are shown in Figure 2. The eye in question is examined to see if it has glaucoma using the DCNN classification method.

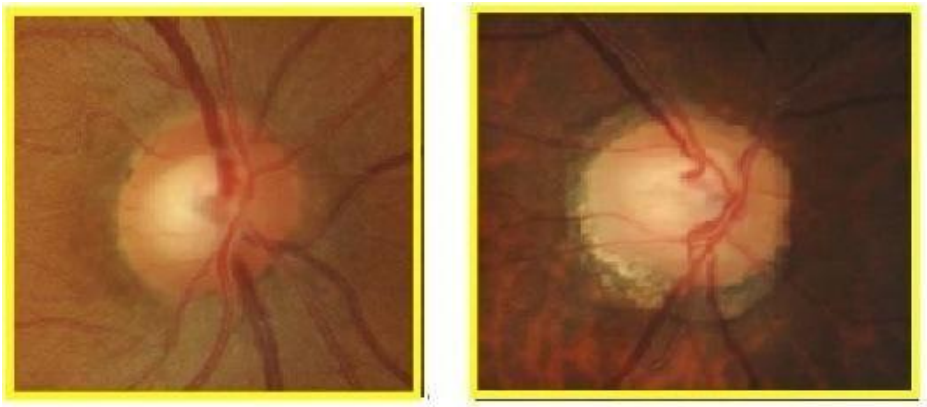

(a) Normal (b) Glaucoma

Fig. 2: Photographs of the optic disc showing a normal disc and optics with varying degrees of glaucomatous optic nerve.

2. BACKGROUND

According to Li et al. (2018), a convolutional neural network (CNN) is a deep learning system that takes an image as input, assigns value to various parts of the image, and performs differentiation among the image set. Convolution neural networks are used in this study to discriminate between images of the eye fundus from glaucoma eyes and normal eyes. A convolution neural network requires far less pre-processing than any other classification algorithm. According to Diaz-Pinto et al. (2019) and Gómez-Valverde et al. (2019), a typical ConvNet consists of numerous convolution layers and filters that can retrieve key information needed for classification. To fine-tune these networks, we need to employ a sizable image data set with more than 14000 images. In 2018, Fu et al. [20] published a deep learning approach for extracting supplementary image-related data and screen glaucoma from fundus pictures. For automated glaucoma screening, a new "disc-aware ensemble network" that integrated the "deep hierarchical context of the fundus image and the optic disc region" was presented. Deep flows were also classified as "global image stream, segmentation-guided network, local disc region stream, and disc polar transformation stream" on various modules and levels.

The benefits are great specificity and accuracy. The key disadvantages are that consumption time is long and it necessitates a greater focus on global information. In 2019, Liao et al. [21] published M-LAP, a unique approach for combining characteristics from various scales to improve the efficacy of glaucoma analysis. Furthermore, the provided strategy produced glaucoma activation, bridging the gap between global semantical analysis and precise locations. It also revealed distinct local locations in fundus images as support for medically interpretable glaucoma analysis. Finally, the results of the investigation revealed the effectiveness of M-LAP in terms of AUC. The EAMNet approach offered the advantage of great sensitivity, which resulted in improved accuracy. The negative was that the optic cup required to be more concentrated, and GAP struggled to display high-resolution feature maps.

A GSO model was provided in 2020 by Jyotika et al. [22], which aided in the automatic identification of optic cups from retinal fundus pictures. The GSO contributed to the creation of a solution by implementing an "intensity gradient within the cup area". By using "adaptive neighbourhoodbehaviour" to extract the searchability of GSO, they were able to detect accurately even when the cup was weak, or the contrast bounds were smaller. The advantages of GSO include decreased error with a high F-score and the drawback of necessitating CDR thought. The main flaw is that at low resolution, the GSO lacks enough pixels to correctly follow the cup limit.

In order to diagnose glaucoma in retinal fundus images, Rutuja Shinde [23] created an "offline Computer-Aided Diagnosis (CAD) model" in 2021. Le-Net architecture was initially used to validate the input data, and the brightest spot algorithm was used to calculate ROI. In addition, U-Net architecture handled the segmentation of the OD and OC. Finally, the Adaboost, NN, and SVM classifiers were used to perform the classification. It benefits from being correct. The lack of consideration for the OCTA image and the incorporation of a small number of characteristics are the drawbacks.

Recurrent U-Net for segmenting the retinal fundus: these tasks increase precision. We compared the two segmentation techniques and assessed the model's accuracy. Patients who underwent both treatments had a memorable experience, as the retinal arteries were separated first, followed by the separation of the optic cup and disc during the second treatment. Both surgeries were carried out on the back of the eyeball. Using the Drishti- GS1 dataset, the model successfully differentiates the optic disc 99.67% of the time and the optic cup 99.50% of the time [24]. Preprocessing is the initial

stage of the image segmentation process, and it must be finished before any segmentation can occur. This was done prior to the segmentation process, which explains why photos taken with the optic cup and disc must be reviewed at this time. Patients who underwent both treatments had a memorable experience, as the retinal arteries were separated first, followed by the separation of the optic cup and disc during the second treatment. Both surgeries were carried out on the back of the eyeball. Using the Drishti- GS1 dataset, the model successfully differentiates the optic disc 99.67% of the time and the optic cup 99.50% of the time [24]. Preprocessing is the initial stage of the image segmentation process, and it must be finished before any segmentation can occur. This was done prior to the segmentation process, which explains why photos taken with the optic cup and disc must be reviewed at this time. These digitally captured retinal pictures might previously have been used to diagnose glaucoma.

This procedure was adopted in many clinical studies, making it the most employed methodology. Any irregularities found during the discovery phase must be removed before analyzing the scan images for further investigation [25,26]. The blood vessels in the image were masked off and exhibited in such a way during the processing step that the final image had no vascular features. In addition, a picture had to be analyzedto properly identify the vast amount of data that had been acquired. The database was modified in this method so that information could be found more quickly and easily. This was done to make the work of sorting through all the data easier. It appears that the goal discussed earlier in the conversation can be realized. When it comes to defining attributes, each technique has a distinct advantage over the others. When conducting data analysis and categorizing items, the image classification method was applied. To be done successfully, this project required a numerical analysis of an image. To complete the investigation on time, the information must be classified as "normal" or "glaucoma." The system should function well thanks to the split optic disc and cup. The machine learning architecture's deep learning capability, which allowed for automated glaucoma detection, was centered on CNN. Researchers employed neural networks that were trained on data from a range of cameras to distinguish between images of the fundus and the optic disc. A variety of final products were created because of the many cameras and lenses that were utilized to take these images [27–29]. The model found that 93% of the 50 photos successfully divided the cup into two parts, and 98% successfully separated the cup from the disc. Images of the retinal fundus were used by Diaz-Pinto et al. to diagnose glaucoma using algorithms developed on ImageNet. This includes ResNet50, VGG-16, and VGG-19. It also includes Xception.

3. METHODS AND MATERIALS

The MATLAB 2015-b platform is used to create the proposed method, and various toolboxes are used for the experiment's software and hardware requirements, including Windows 10 OS, Core i3-4130 3.40GHz Processor, 4GB RAM, 1TB (1000 GB) Hard Drive, ASUSTek P5G41C-M Motherboard, and Internet Protocol. Training and validation databases are two separate sets that make up the DRISTI database. For each dataset, 70% of the photos are used for training and the remaining 30% are used for validation. The runtime is the length of time needed for the algorithm to execute, and it depends on the CPU execution time, processor speed, instruction set, disc speed, and compiler manufacturer.

3.1 Datasets and Evaluation Metrics for Retinal Disease Diagnosis

Fundus photography is the process of obtaining a two-dimensional image of the three-dimensional ocular retinal fundus by projecting reflected light onto an image plane. The most well-known open access fundus photo datasets were categorized and used. We used 661 fundus photos [31], 224 normal images, and 137 glaucoma images in our study. The images are saved in JPEG format using

the fundus camera's built-in imaging software. The image resolution was 560 x 720 pixels. All data samples were obtained from publicly available online datasets. Patients with primary open-angle (either high- or low-tension glaucoma), pseudo exfoliative, or pigmentary glaucoma were included in the study. Clinically, glaucoma patients were identified based on the presence of specific structural changes on dilated stereoscopic examination of the optic nerve head, such as increased cup-to-disc ratio, cup-to-disc ratio asymmetries, localized or generalizedneuroretina rim thinning or notching, deepening of the optic cup, and glaucomatous disc hemorrhages, with or without concordant visual field defects on conventional white on-white standard automated perimetry. The four crucial aspects of the developed glaucoma detection approach are (i) pre-processing, (ii) optic cup segmentation, (iii) feature extraction, and (iv) detection. The input image is pre-processed using a GF. Using the filtering procedure enhances the image's quality. The Modified Level Set Algorithm is used for optic cup segmentation with the original image size being (1152, 1500, 3), and the downsized image size being (256, 256, 3). The feature extraction step uses two different kinds of characteristics. Both morphological and non-morphological traits are present. Then, morphological features (Femf) like disc area, cup area, and RNFL thickness are extracted along with non-morphological features (Fenmf) including color, form, and Modified LBP utilizing closing and dilation operations. The optimized CNN receives these features and adjusts the weights using a suitable tuning technique. The image of the glaucoma detection model is depicted in Fig. 3.

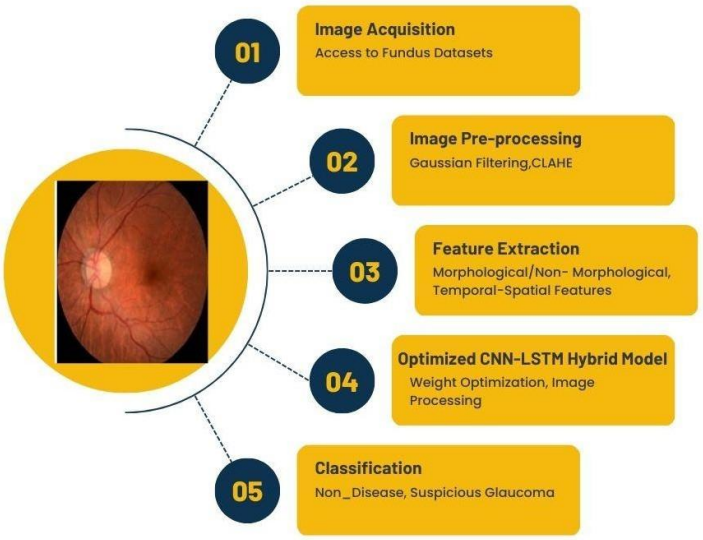

Fig. 3: Proposed System for Glaucoma Detection using Deep Learning Model.

3.2 Deep Learning Concepts

Deep learning (DL) is a type of artificial intelligence technology based on artificial neural networks (learning methods influenced by the biological structure of the human brain). The latent and intrinsic relationship of the input data is automatically learned in the DL process using mathematical representations. Unlike typical machine learning (ML) methods, deep learning (DL) can run with significantly less human guidance since it extracts relevant characteristics from data without relying on hand-crafted features. This qualifies DL for medical image analysis, where features can be learned automatically from complex visual data. The designs of some of the most employed backbone models, particularly for classification and segmentation tasks in retinal disease diagnosis, are discussed in the following section.

3.3 Backbone Models for Classification Task

There are numerous backbone models that can be utilized for glaucoma detection categorization. Here are a few examples. Using transfer learning, these backbone models can be fine-tuned for the glaucoma classification job. The last fully connected layer of the pre-trained model is replaced with a new layer that outputs the appropriate number of classes, and the network is then trained using the glaucoma classification dataset.

3.3.1 Convolution Neural Networks (CNN)

A convolution neural network (CNN) is one of the most often utilized DL designs for effective training across several layers [32]. CNN is made up of three main parts: convolution layers, pooling layers, and fully connected layers. There are two parts to the training procedure. The first stage, known as the forward stage, involves representing the input image with the proper weights and biases in each layer, and then using the anticipated output to calculate the loss function by comparing it against values from the ground truth. The gradients of each parameter are calculated based on the loss function in the second stage, sometimes referred to as the backward stage. After then, the parameters are revised and set up for the following forward stage. Multiple iterations of this are performed until the network produces accurate classification results. The fundamental CNN Architecture Pipeline is shown in Figure 4. CNN categorization often requires multiple phases, including:

• Data Preparation: The initial stage in the process is to categorize and divide the training data into training and validation sets.

• Model Definition: A CNN model is then described, consisting of pooling layers, fully connected layers, and one or more convolutional layers.

• Model Training: Using training data, the model is trained, and an optimization approach like Stochastic Gradient Descent (SGD) is used to update the CNN's weights.

• Model Evaluation: The validated data from the trained model is then used to evaluate the trained model's correctness and pinpoint any overfitting or underfitting issues.

• Prognosis: After training and testing, the model can be used to categorize new photos into the relevant groups.

Overall, CNN classification is a potent method for categorizing images automatically into several groups, and it has a wide range of real-world uses in industries including computer vision, medical imaging, and robotics.

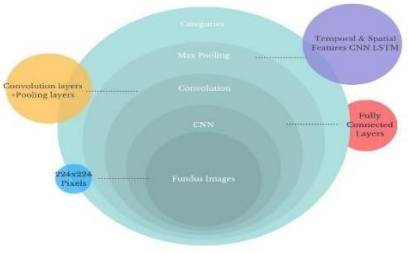

Fig. 4: Venn diagram for visualizing the architecture of a CNN.

3.3.2 VGGNet

VGG Network (VGGNet) is another often utilized backbone network in the classification of retinal diseases. In 2014, Karen Simonyan and Andrew Zisserman made this suggestion [33]. From VGG-16 to VGG-19, the Visual Geometry Group (abbreviated VGG) produced numerous iterations of Convolution network models for various image categorization applications. VGG was initially designed with the goal of investigating how CNN depth affects picture categorization accuracy. All layers of the model employ a modest 3 * 3 kernel to enhance network depth without using an excessive number of parameters. The input size for VGGNet is a 224*224 RGB picture. A fixed convolution step is combined with a 3 * 3 filter. Due to the three completely connected layers, the total number of convolutions plus fully connected layers can range from VGG-11 to VGG-19. Eight convolution layers precede three completely connected layers in VGG-11. In contrast, VGG-19 has three completely connected layers and sixteen convolution layers. In VGGNet, there are a total of five pooling layers scattered across the network rather than one pooling layer being added after each convolution layer.

3.3.3 ResNet.

Residual network (ResNet) [34] has 152 layers that are formed by stacking individual residual blocks). These residual blocks are made up of two convolution layers (3 * 3). The number of filters is doubled on a regular basis and spatially down sampled with a stride of 2. After each convolution layer, this network includes unique skip connections as well as batch normalization. Skip connections are used to optimize deep models since they take activation from one layer and feed it immediately to another. This has the effect of allowing deep neural networks to be trained without facing vanishing gradient difficulties. ResNet has a fully connected layer that outputs 1000 classes to reduce the number of parameters.

3.3.4 Extracting temporal features from retinal Images.

Recurrent neural networks (RNN) are specifically developed to recognize patterns in data sequences or, in our case, photographs. All inputs in a typical neural network are viewed as independent of one another. The disadvantage of such a technique is in jobs that require the network to remember events from past data, such as predicting a frame in a video. RNNs are referred to as recurrent because they do the same duty for each element in a sequence. The output of these networks is determined by earlier computations. Furthermore, these networks feature a "memory" that stores information about previous calculations. Long Short-Term Memory (LSTM) is the most widely used RNN network. Its better performance in language translation and audio processing has made it the primary RNN of choice for jobs requiring feature extraction from a sequence of data (e.g., movies). The LSTM architecture is made up of memory blocks, each of which has several memory cells. Each memory cell is made up of three gates: forget, input, and output. The forget gate is a function that determines which information to keep and which to discard. The input gate determines what new data will be stored in each cell. The output gate picks and displays valuable information from the current cell state. The overall framework of the fused Convolutional Neural Network-Recurrent Neural Network (CNN-RNN) is depicted in Figure 5. The temporal features are created by passing the retrieved spatial features from CNN through the RNN.

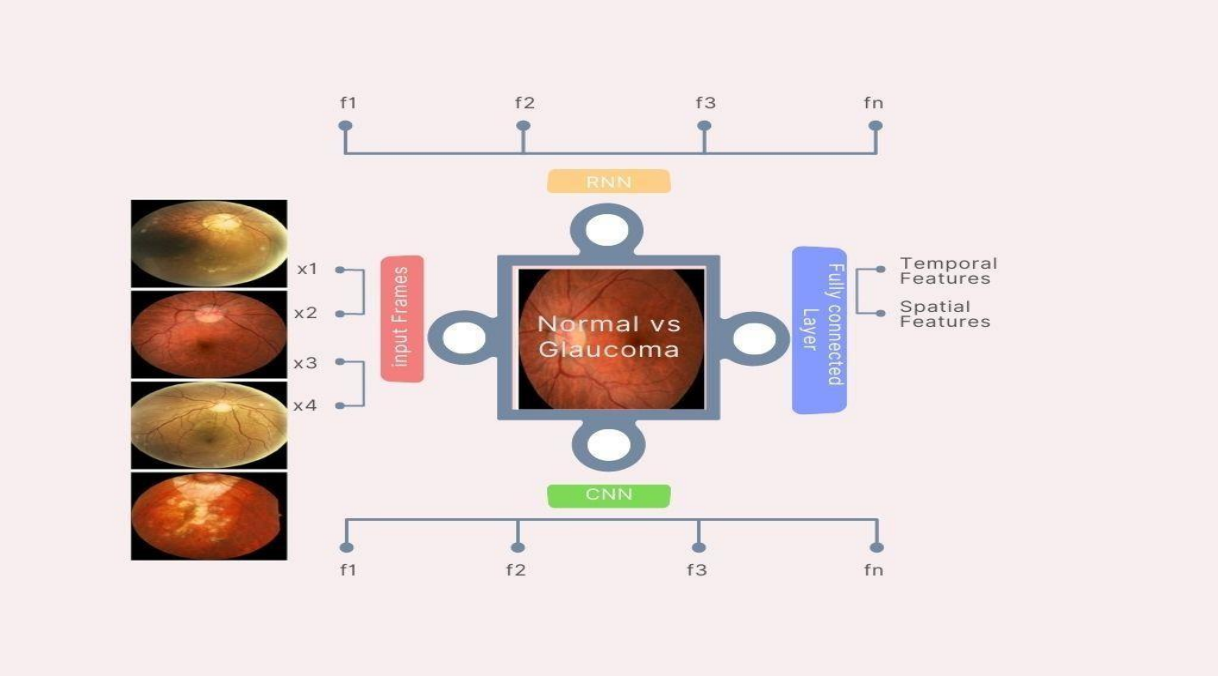

Fig. 5: Overall Framework of the Fused Convolutional Neural Network-Recurrent Neural Network (CNN-RNN).

4. RESULTS AND DISCUSSION

We are going to employ transfer learning to retrain CNN LSTMNetto create glaucoma illness prediction software. For this, we load the pre-trained LSTMNet network as well as the several image databases that contain the images of the various pathologies that need to be diagnosed, such as glaucoma. The fresh photos need to be loaded in Image data format after being unzipped and unzipped before starting training with this new dataset. According to the folder names, LSTMNet will automatically identify the images as non-disease fundus eyes images, glaucoma fundus eyes images, and retinopathy fundus eyes images. The data must then be split into training and validation data sets before the model stores it as an image data object. Once the initial classification is made, the model divides the data further into training images (corresponding to 70% of the images) and validation images (equal to 30% of the images). To do this, we use the "splitEachLabel" function, which divides the images data store into two new data stores.

4.1 Preprocessing

Gaussian filtering is used as a preprocessing step on the input image. Filtering is required to create high-quality images. GF [32], It is used to remove noise from an image that has blurred because of the image's higher frequency components getting smaller. The GF filter could be used to eliminate Gaussian noise from brain MR pictures or speckle-noise images in an Ultra-Sound image. In this method, the noisy pixel of the image is replaced by the mean neighbor pixel value. A 5 5 window size is used in the Gaussian denoising method. Fundus images are typically pre-processed before the training phase to enhance the training process and create reliable prediction models. This is done to make up for the noise that was brought on by the various image-capture gear employed in the different imaging lighting conditions. Due to the intricacy of the retinal structure and the low picture quality, many significant biomarkers and lesions may go undetected. Before DL model implementation, pre-processing techniques are employed to improve the fundus picture attributes in

addition to reducing undesired noise One of the writers (SG) normalized all the images and frames before marking the optic disc's center in each frame of each film. This was done before creating the deep leaning architecture. Then, using an automatic method, all images were reduced to a square area with the optic disc in the center and no more than two disc diameters around the manually marked disc center. This strategy was chosen because the retinal tissue around the ONH mostly exhibits glaucoma-specific static and dynamic characteristics. When training CNNs, clipping images around the optic disc is more effective than using the entire image.[35] Finally, to address the imbalance problem in our dataset and boost the number of normal photos, we used a data augmentation technique in the training set. The training images were improved by randomly rotating, zooming, and flipping them horizontally. We scaled the images to comply with this criterion as the network's default input image size is 224 224. The fundus image filtering procedure is shown in Figure 6.

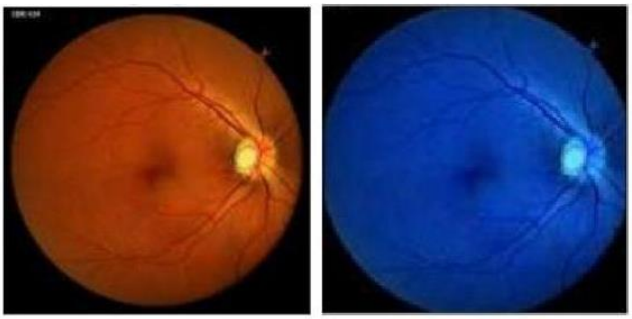

(a) Original Fundus Image (b) Filtered Image
Fig. 6: Preprocessing stage applying filters.

4.2 Optic cup segmentation

The optic cup is the bright yellowish circular area in the center of the optic disc. One of the most challenging tasks is cup detection from a fundus image since the color intensity of the cup region is like that of the Optic disc region, making cup detection challenging. Additionally, because all blood vessels originate from the optic nerve, which is situated in the center of the optic disc, the blood vessels in the cup region are blocked. The vessels obscure the cup region, yet small portions of the cup can be seen inside the optic disc. The optic cup is the bright yellowish circular area in the center of the optic disc. One of the most challenging tasks is cup detection from a fundus image since the color intensity of the cup region is like that of the Optic disc region, making cup detection challenging. Additionally, because all blood vessels originate from the optic nerve, which is situated in the center of the optic disc, the blood vessels in the cup region are blocked. The vessels obscure the cup region, yet small portions of the cup can be seen inside the optic disc. The level set segmentation algorithm is changed to address some flaws. Edge-oriented and region-oriented schemes are the two categories into which the level set technique is divided [30]. The "Modified Level Set segmentation" algorithm is employed to segment the optic cup. Both edge-oriented and region-oriented techniques are taken into consideration in the modified level set segmentation. Equations 1 and 2 were utilized to test the proposed model's specificity and sensitivity.

$$\textbf{Sensitivity (tpr)} = tp/(tp + fn) \quad (1)$$

$$\textbf{Specificity (tnr)} = tn/(tn + fp) \quad (2)$$

4.3 Combining CNN and RNN-Network Training.

To extract spatial and temporal information, we created an architecture that combines CNN (VGG16 and ResNet 50) and RNN (LSTM). To extract spatial information, each image set is

divided into consecutive images and fed into CNN. The outputs are then used to detect temporal properties in the image sequence by feeding them into a recurrent sequence learning model (LSTM). Finally, a fully linked layer receives the aggregated characteristics to forecast the classification for the entire input sequence. Using transfer learning, we assessed the networks previously presented. Model weights are initialized based on the ImageNet dataset, a sizable benchmark dataset for object category classification and detection on hundreds of object categories and millions of photos, in transfer learning as opposed to native training. Except for the fully connected layers, which are trained on our created fundus dataset, transfer learning is used to initialize the model weights based on a sizable general picture dataset. We partitioned the dataset into three subsets at random for training and evaluation purposes: training (85% of the total images), testing (10% of the total images), and validation (5% of the total images). We also calculated the F-measure, precision, and recall. The average F-measures, precisions, and recalls are presented after this technique was repeated ten times. All pictures and videos from a single participant were included in the same subset to guarantee a uniform training and testing process. In other words, throughout the training and validation phases, not all the images and videos used to test the network were "seen" by the network. Figures 9 and 10 show proposed model graphs, Figures 7 forecasts model prediction, Figure 8 depicts the venn diagram for model prediction using the LSTMNet model, and Table 1 formulates the performance of various models on the combined datasets of the DIARETDB0[36], ACRIMA [37], DRISTI, and Retina image bank database [38]. Performance of the various models on the entire dataset is shown in Table 2.

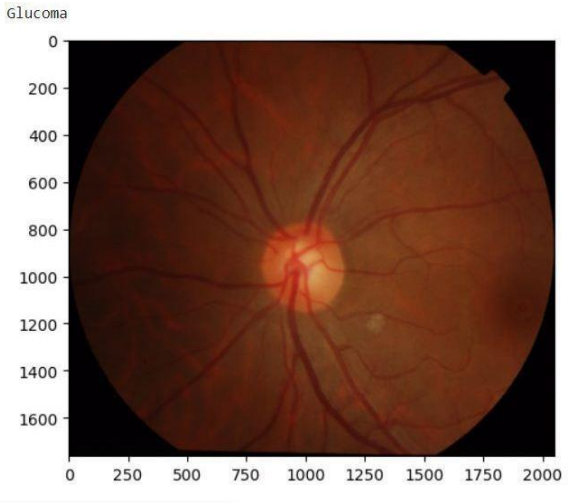

Fig. 7: Model Prediction.

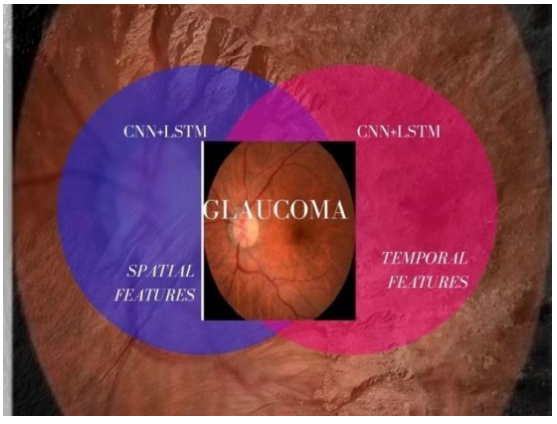

Fig. 8: Venn diagram for LSTMNet Model Prediction

Table 1: Comparison of the testing and training accuracy of the proposed model with traditional models.

Model	Training	Testing
VGG-19	97.72	95.55
Inception ResNet	94.85	91.60
ResNet 152v2	97.54	93.20
DenseNet169	97.15	95.46
U-Net	98.10	96.30
Proposed	98.21	96.34

Table 2: Performance of the various models on the total dataset.

Models	Sensitivity	Specificity	F-measure (%)
CNN			
VGG16	0.61	0.65	71%
Resnet_N	0.71	0.76	79.5%
CNN+RNN			
VGG16+LSTM	0.96	0.97	96.21%
Resnet_N+LSTM	0.90	0.97	93.2%
Proposed	0.91	0.98	94.06%

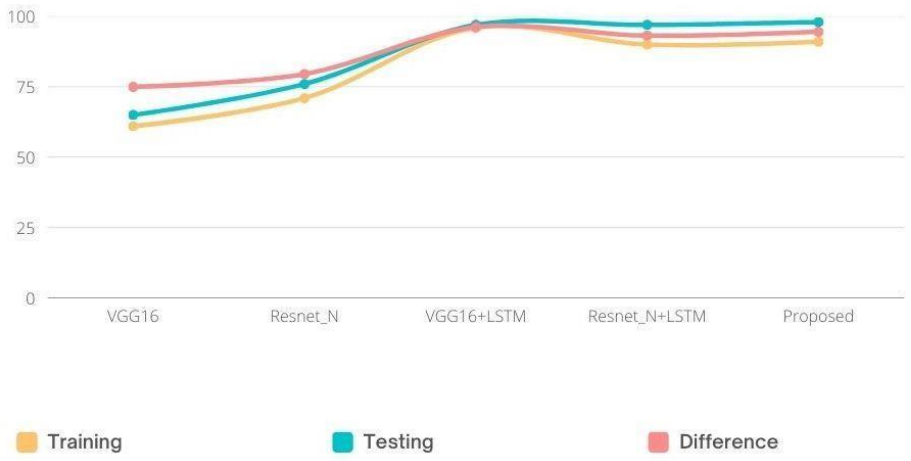

Fig. 9: Performance of the various models on the total dataset graph.

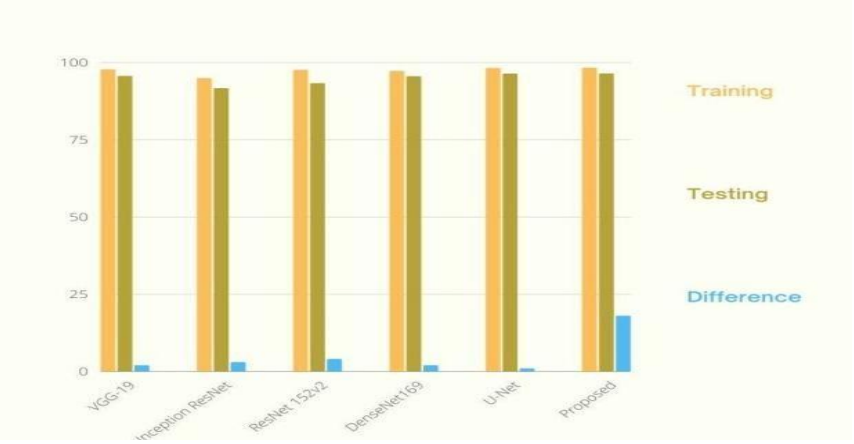

Fig. 10: Comparative analysis of recall of the proposed model with tradition

5. CONCLUSION AND FUTURE SCOPE.

In this study, deep learning is suggested as a revolutionary technique for glaucoma diagnosis and prediction. The glaucoma image analysis deep learning model was trained using the glaucoma dataset. A deep convolutional neural network was used to classify the images to develop a CNN-LSTMNet technique for glaucoma detection. The patient's glaucoma status was determined using these retinal fundus pictures. The optic cup region was extracted from the fundus photographs, and the extracted image data was then compared to the ground truth images in the dataset. Early on, picture pre-processing is done to improve image quality by de-noising the input image. For illness identification, the color, texture, and intensity properties are retrieved more accurately. The segmentation of the feature extraction images takes these retrieved features into account. The developed algorithm divides the pixels into groups in picture space by determining the local maxima modes of each pixel. The distance between two segmented sections is used to categorize these segmented images. Images of the retinal fundus are then categorized. This improves the diagnosis of diseases. Compared to DCNN's OD localization approach, the method's outcome increases illness detection accuracy with less time and error. The findings of this study might apply to a few imaging modalities. Another advantage of the suggested transfer learning method is that it can be used in a range of contexts, including but not limited to manufacturing, transportation engineering, industrial imaging, and other fields. Future attempts will use semi-supervised and fuzzy approaches.

The suggested approach is then put into practice to increase accuracy and cut down on time by utilizing cutting-edge deep learning methods, for further study in this area, using deep learning techniques to large-scale fundus photo benchmarks seems to be a viable direction. The lack of publicly accessible picture benchmarks has also been noted, and many researchers employ their own fundus image benchmarks to assess the quality of their own work. To assess future research in this area, a large, easily accessible image standard must be developed. This will be important in determining the best performance of future experiments based on the same data set and in developing an efficient CAD for glaucoma detection.

6. FINANCIAL DISCLOSURE

This research received no external funding.

INSTITUTIONAL REVIEW BOARD STATEMENT

Not applicable.

INFORMED CONSENT STATEMENT

Not applicable.

CONFLICTS OF INTEREST

The authors declare no conflict of interest.

AUTHOR CONTRIBUTIONS

Conceptualization, methodology, software validation, resources, writing-original draft preparation, Writing-review and editing, visualization was carried out by Prof. Santhosh S, all authors have read and agreed to the published version of the manuscript.

ACKNOWLEDGEMENTS

I wish to thank my parents for their support and encouragement throughout my studies.

References

1. Tham YC, Li X, Wong TY, et al. Global prevalence of glaucoma and projections of glaucoma burden through 2040: a systematic review and meta-analysis. Ophthalmology. 2014;121:2081–2090.
2. Lee EB, Wang SY, Chang RT. Interpreting deep learning studies in glaucoma: unresolved challenges. Asia Pac J Ophthalmol (Phila). 2021;10:261–267.
3. Quigley, H. A., Brown, A. E., Morrison, J. D. &Drance, S. M. The size and shape of the optic disc in normal human eyes. Arch. Ophthalmol. 108(1), 51–57 (1990).
4. Jonas, J. B., Zäch, F. M., Gusek, G. C. & Naumann, G. O. Pseudoglaucomatous physiologic large cups. Am. J. Ophthalmol. 107(2), 137–144 (1989).
5. Wiley, H. &Iii, F. Nonproliferative diabetic retinopathy and diabetic macular edema. Retina Fifth Edn. 2, 940–968 (2012).
6. Spaeth, G. L. et al. The disc damage likelihood scale: Reproducibility of a new method of estimating the amount of optic nerve damage caused by glaucoma. Trans. Am. Ophthalmol. Soc. 100, 181–186 (2002).
7. A. S. M and N. Thillaiarasu, "A Survey on Different Computer Vision Based Human Activity Recognition for Surveillance Applications," 2022 6th International Conference on Computing Methodologies and Communication (ICCMC), Erode, India, 2022, pp. 1372-1376, doi: 10.1109/ICCMC53470.2022.9753931.
8. Flammer, J. et al. The impact of ocular blood flow in glaucoma. Prog. Retina Eye Res. 21(4), 359–393. https ://doi.org/10.1016/s1350-9462(02)00008 -3 (2002).
9. Golzan, S. M., Graham, S., Leaney, J. & Avolio, A. Dynamic association between intraocular pressure and spontaneous pulsations of retinal veins. Curr. Eye Res. 36, 53–59. https ://doi.org/10.3109/02713 683.2010.53073 1 (2011).
10. Morgan, W. H. et al. Photoplethysmographic measurement of various retinal vascular pulsation parameters and measurement of the venous phase delay. Investig. Ophthalmol. Vis. Sci. 55(9), 5998–6006. https ://doi.org/10.1167/iovs.14-15104 (2014).
11. Golzan, S. M., Morgan, W. H., Georgevsky, D. & Graham, S. L. Correlation of retinal nerve fibre layer thickness and spontaneous retinal venous pulsations in glaucoma and normal controls. PLoS ONE 10(6), 1–12. https ://doi.org/10.1371/journal.pone.0128433 (2015).
12. Golzan, S. M., Georgevsky, D., Bowd, C., Weinreb, R. & Graham, S. Visual field sensitivity is decreased with reduced spontaneous venous pulsation in glaucoma eyes. Investig. Ophthalmol. Vis. Sci. 58(8), 734 (2017).
13. S. K. A. S, S. S, A. S. M and S. K. S, "Machine Learning based Ideal Job Role Fit and Career Recommendation System," 2023 7th International Conference on Computing Methodologies and Communication (ICCMC), Erode, India, 2023, pp. 64-67, doi:

10.1109/ICCMC56507.2023.10084315.

14. Cheriguene, S., Azizi, N., Djellali, H., Bunakhla, O., Aldwairi, M. and Ziani, A. New computer aided diagnosis system for glaucoma disease based on twin support vector machine. In International Conference on Embedded Distributed Systems (EDiS), pp. 1–6,(2017).
15. Al-Bander, B., Al-Nuaimy, W., Al-Taee, M. A. and Zheng, Y. Automated glaucoma diagnosis using deep learning approach. In 14th International Multi-Conference on Systems, Signals & Devices (SSD), pp. 207–210 (2017).
16. Christopher, M. et al. Performance of deep learning architectures and transfer learning for detecting glaucomatous optic neuropathy in fundus photographs. Sci. Rep. https ://doi.org/10.1038/s4159 8-018-35044 -9 (2018).
17. Diaz-Pinto, A., Morales, S., Naranjo, V., Thomas, K. &Mossi, J. M. CNNs for automatic glaucoma assessment using fundus images:An extensive validation. BioMed. Eng. 18(29), 1–19. https ://doi.org/10.1186/s1293 8-019-0649-y (2019).
18. Wiley, H. &Iii, F. Nonproliferative diabetic retinopathy and diabetic macular edema. Retina Fifth Edn. 2, 940–968 (2012).
19. Li, L.; Xu, M.; Liu, H.; Li, Y.; Wang, X.; Jiang, L.; Wang, Z.; Fan, X.; Wang, N. A large-scale database and a CNN model for attention-based glaucoma detection. IEEE Trans. Med. Imaging 2020, 39, 413–424.
20. Fu H, et al. Disc-aware ensemble network for glaucoma screening from fundus image. IEEE Trans Med Imaging 2018;37(11):2493–501. https://doi.org/10.1109/ TMI.2018.2837012. Nov.
21. Vaishali, M. Ashwin Shenoy, P. R. Betrabet and N. S. Krishnaraj Rao, "Helmet Detection using Machine Learning Approach," 2022 3rd International Conference on Smart Electronics and Communication (ICOSEC), Trichy, India, 2022, pp. 1383-1388, doi: 10.1109/ICOSEC54921.2022.9952083.
22. PruthiJyotika, Khanna Kavita, Arora Shaveta. Optic Cup segmentation from retinal fundus images using Glowworm Swarm optimization for glaucoma detection. Biomed Signal Process Control 2020;60:102004. Cover date: July 2020), Article 102004, 19 May.
23. Shinde Rutuja. Glaucoma detection in retinal fundus images using U-Net and supervised machine learning algorithms. Intell-Based Med 2021;5.
24. Jiang, Y.;Wang, F.; Gao, J.; Cao, S. Multi-path recurrent U-Net segmentation of retinal fundus image. Appl. Sci. 2020, 10, 3777.
25. Diaz-Pinto, A.; Morales, S.; Naranjo, V.; Köhler, T.; Jose, M.; Navea, A. CNNs for automatic glaucoma assessment using fundus images: An extensive validation. BioMed. Eng. Online 2019, 18, 29.
26. SynaSreng, N.M.; Hamamoto, K.; Win, K.Y. Deep learning for optic disc segmentation and glaucoma diagnosis on retinal images. Appl. Sci. 2020, 10, 4916
27. Nair, R.; Bhagat, A. An Application of Big Data Analytics in Road Transportation. In Advances in Systems Analysis, Software Engineering, and High Performance Computing; IGI Global: Hershey, PA, USA, 2018; pp. 39–54.
28. Nair, R.; Bhagat, A. An Introduction to Clustering Algorithms in Big Data. In Encyclopedia of Information Science and Technology, 5th ed.; IGI Global: Hershey, PA, USA, 2021; pp. 559–576.
29. A. S. M, S. S and S. K. S, "A Study on various Applications of Computer Vision for Teaching Learning in Classroom," 2022 6th International Conference on Electronics, Communication and Aerospace Technology, Coimbatore, India, 2022, pp. 896-900, doi: 10.1109/ICECA55336.2022.10009136.
30. Huang Juying, Jian Fengzeng, Wu Hao, Li Haiyun. An improved level set method for

vertebra CT image segmentation. Biomed Eng Online 2013;12:48. https://doi.org/10.1186/1475-925X-12-48.

31. J. Hu, M. Bhaskaranand, J. Gibson, Rate distortion lower bounds for video sources and the HEVC standard, in Information Theory and Applications Workshop (ITA) (2013), pp. 1–10
32. Y. LeCun, L. Bottou, Y. Bengio, and P. Haffner, ``Gradient-based learning applied to document recognition," Proc. IEEE, vol. 86, no. 11, pp. 2278_2324, Nov. 1998.
33. S. S and D. V. Babu, ``A Critical Review on Ophthalmic Diagnosis of Glaucoma in Fundus Images of Eye using Deep Learning Models," 2023, Unique Paper ID: 157443,Publication Volume & Issue: Volume 9, Issue 7, Page(s): 261 - 264.
34. K. He, X. Zhang, S. Ren, and J. Sun, ``Deep residual learning for image recognition,' in Proc. IEEE Conf. Comput. Vis. Pattern Recognit. (CVPR), Jun. 2016, pp. 770_778.
35. Orlando, J., Prokofyeva, E., Fresno, M., and Blaschko, M. Convolutional neural network transfer for automated glaucoma identification. In International Symposium on Medical Information Processing and Analysis, pp. 241–250 (2017).
36. S. S and D. V. Babu, "Retinal Glaucoma Detection from Digital Fundus Images using Deep Learning Approach," 2023 7th International Conference on Computing Methodologies and Communication (ICCMC), Erode, India, 2023, pp. 68-72, doi: 10.1109/ICCMC56507.2023.10083712.
37. ACRIMA.database,https://figshare.com/articles/CNNs_for_Automatic_Glaucoma_Assessment_using_Fundus_Imags_An_Extensive_Validation/7613135, 2019
38. Retina image bank database, https//magebank.asrs.org/file/28619/stargardt-disease, 2018